DETECTING ABNORMAL FEED RATE IN ALUMINIUM ELECTROLYSIS USING EXTENDED KALMAN FILTER

Kristin Hestetun and Morten Hovd *

** Department of Engineering Cybernetics,
Norwegian University of Science and Technology,
N-7491 Trondheim, Norway*

Abstract: One factor influencing the current efficiency in an aluminium electrolysis cell is the concentration of dissolved alumina in the electrolyte. Unfortunately, no direct measurement of alumina concentration is usually available and present control strategies for alumina feed control rely heavily on the change in cell pseudo-resistance. This paper describes work done to investigate the possibility of using additional measurements of anode current distribution in an extended Kalman filter for the purpose of detecting malfunctioning alumina feeders. *Copyright © 2005 IFAC*

Keywords: Extended Kalman Filter, parameter estimation, fault detection.

1. INTRODUCTION

The energy efficiency in an aluminium electrolysis cell depends on several factors, one being the concentration of dissolved alumina in the electrolyte. Both too high and too low concentration of alumina may lead to serious operational problems. One such problem is the so-called anode effect which occurs at low alumina concentrations. However, the control of alumina concentration is not very accurate because of the limited process information that is available online. Frequent measurements of key control variables like temperature and concentration of alumina in the electrolyte are in general not available. Present control strategies are based mainly on measurements that can be obtained from the outside of the cell, in practice change in cell pseudo-resistance which is calculated from the measured line amperage and total cell voltage drop. No cost efficient sensors for measuring alumina concentration for industrial use have yet been developed. According to Bearne (1999) it is probable that the change in pseudo-resistance with alumina concentration will con-

tinue to be used for control for many years. On these premises, any additional measurements that can give insight into how alumina is distributed in the cell may help improve alumina feed control and reduce spatial variation within the cell.

Motivated by the observations made by Rye *et al.* (1998) this paper investigates the possibility of using measurements of anode current distribution to help detect and if possibly identify the cause of abnormal alumina addition and distribution in the cell. At low alumina concentration, Rye *et al.* (1998) found that anodes located in areas where the alumina concentration was low took less current than anodes in areas where the alumina concentration was higher. A previous paper (Jakobsen *et al.*, 2001) describes work done to estimate alumina concentration profiles based on measured cell voltage drop and anode current distribution. Here the focus is on detecting faulty feed rate using data from anode current distribution and total cell voltage drop.

2. PROCESS DESCRIPTION

Aluminium is produced by electrochemical reduction of aluminum oxide (Al_2O_3, also called alumina) dissolved in a liquid electrolyte at temperatures close to $1000°C$. A sketch of a modern electrolysis cell is given in Fig. 1. The cells studied in this work have 18 prebaked anodes arranged in two rows and connected in parallel to the horizontal bus bars. The anodes are partly submerged in the liquid electrolyte which consists mainly of molten cryolite (Na_3AlF_6), excess aluminium fluoride (AlF_3) and alumina. The DC electrolysis current enters the cell through the bus bars and is distributed among the individual anodes. As the high amperage current passes through the electrolyte and into the cathode, liquid aluminium is formed at the metal/bath interface acting as the cathode while carbon-oxide gases are produced at the anodes. The main cell reaction is given as

$$Al_2O_{3(diss)} + \frac{3}{2}C_{(s)} \rightarrow 2Al_{(l)} + \frac{3}{2}CO_{2(g)} \quad (1)$$
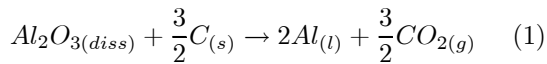
The anode carbon is consumed in the reaction so the individual anodes have to be replaced at regular intervals, about once a month.

The alumina is fed to the electrolyte through two point feeders, one in each end of the cell. Because the electrolyte is covered by a layer of frozen electrolyte and alumina powder, each feeding operations implies making a hole in the top crust with a bar and allowing a controlled amount of alumina powder to be dropped into and dissolved in the electrolyte. If the concentration of dissolved alumina in the electrolyte drops below a critical level, an anode effect may arise. During anode effect, depletion of alumina underneath the anodes causes the resistance (and cell voltage) to increase dramatically without any corresponding increase in metal production. In addition to giving low energy efficiency and disturbing the cell energy balance, anode effect causes production of significant amounts of CFC gases, which are harmful to the environment and have a very strong "greenhouse effect". At the same time, addition of too much alumina may lead to sludge formation as undissolved alumina is deposited at the cathode surface. Faulty equipment, for example a leak in one of the feeders or a malfunctioning bar, could mean that the amount of alumina that is actually dissolved in the electrolyte is considerably different from what is assumed by the process control system. If this situation goes on unnoticed over time, it may eventually lead to an unwanted anode effect or sludge problems.

The voltage drop between the anode-bus bar contact point and the cathode is the same for all anodes in a cell. According to Ohm's law, more
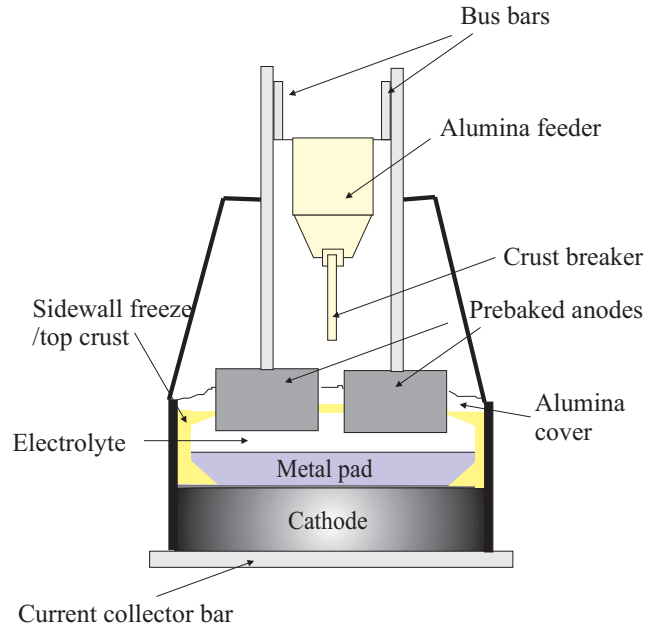

Fig. 1. An illustration of a prebake aluminium electrolysis cell, as seen from the shorter side.

current will go where there is less resistance, and the way the current distributes between the individual anodes depend upon the resistance in the anodes and in the inter-electrode gap. Because anode resistance is fairly constant over time, and resistance in the electrolyte strongly depends on alumina concentration, the anode current distribution should give information about alumina distribution and concentration in the cell.

3. PROCESS MODELING

In (Jakobsen *et al.*, 2001) a model for estimation of alumina concentration profile in an aluminium electrolysis cell was presented. The cell was divided into 18 control volumes, one for each anode, and a nonlinear state space model for estimation of alumina concentration in each control volume was developed from mass balances and known physical and empirical relations. Here, the objective is to detect abnormal changes in alumina concentration between different parts of the cell and hence the detailed distribution of alumina in the cell is not so important.

Based on the model presented in (Jakobsen *et al.*, 2001), a simplified model is developed where the number of control volumes is reduced to three, all assumed to contain the same volume of electrolyte. Undissolved alumina is fed to the cell, and the rate of dissolution of alumina is assumed to be proportional to both the concentration of undissolved alumina and the degree of under-saturation of dissolved alumina in the electrolyte. The rate of metal production (and alumina consumption) is given by Faraday's law and the cell current efficiency factor. Mass transport of both undis-

solved and dissolved alumina between adjacent control volumes are described by dispersion. Neglecting all temperature variations, the resulting state space model derived from the mass balance of undissolved and dissolved alumina and change in anode-cathode distance can be written as

$$\dot{x} = f(x, u, \theta) \qquad (2)$$
$$y = g(x, u)$$

Here both f and g are nonlinear functions. For each control volume, the state vector $x = \begin{bmatrix} \psi & c & \delta \end{bmatrix}^T$ where ψ and c are the concentration of undissolved and dissolved alumina respectively, and δ is the anode-cathode distance. The parameter vector $\theta = \begin{bmatrix} k_{1\rightarrow2} & k_{2\rightarrow3} & k_{mtf} & M_e \end{bmatrix}$ where $k_{1\rightarrow2}$ and $k_{2\rightarrow3}$ are dispersion parameters, k_{mtf} is the mass transfer coefficient for dissolution of alumina and M_e is the mass of electrolyte in each control volume. The model inputs $u = \begin{bmatrix} F1 & F2 & ACD & I_1 & I_2 & I_3 \end{bmatrix}$ are the feed rate alumina for the two point feeders, the change in anode-cathode distance and the anode currents through the three sections in the cell.

Fig. 2 shows the layout of the cells studied. The two dispersion coefficients, $k_{1\rightarrow2}$ and $k_{2\rightarrow3}$, the mass transfer coefficient k_{mtf} and the mass of electrolyte in a control volume M_e are unknown and must be estimated from experimental data.

The measurement vector, y, consists of the calculated total cell voltage drop and the estimated alumina concentration for each control volume. The total cell voltage drop consists of several terms, some of which depend on the alumina concentration. The equations for calculation of y are found from literature data (Solheim,1998; Haupin, 1998).

4. EXPERIMENTAL

The model is validated against three experimental data sets collected from industrial working electrolysis cells at Elkem Aluminium ANS' plant in Mosjøen, Norway. Normal cells with no indications of abnormal process conditions were chosen for the experiments. Thus, the measurements are assumed to be corrupted with the normal amount of process and measurement noise. The experiments involved introducing rather large changes in normal feed rate at the same time as anode current distribution and cell voltage were logged. During the time of feed disturbance, also the concentration of alumina in the electrolyte and electrolyte temperature were measured at regular intervals at six positions in the cell (see Fig. 2).
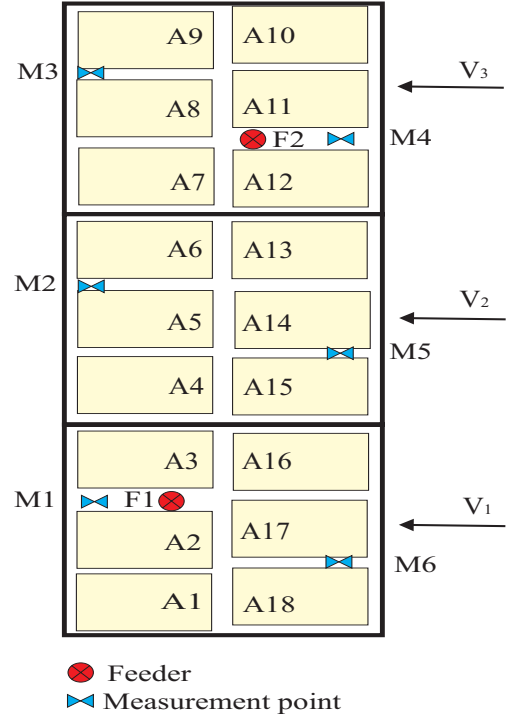
The experiments considered here are:

Fig. 2. Layout of the prebake electrolysis cells where the experiments were performed. Placement of anodes (A), control volumes (V), feeders (F) and measurement points (M) are indicated.

- *Experimental run 1*: Feeder in position F1 was closed down at the end of an underfeeding period. The total cell feed rate was kept at 50% of normal feed rate until anode effect arose.
- *Experimental run 2*: Both feeders in the cell were closed down at the end of an overfeeding period. The feeding was stopped until anode effect arose.
- *Experimental run 3*: Normal feed cycle. A period of overfeeding (more than theoretical consumption rate) followed by a period of underfeeding (less than theoretical consumption rate). The cell was kept at underfeeding until anode effect arose.

5. ESTIMATION

5.1 Parameters and initial conditions

The parameter vector θ and the initial conditions x_0 were estimated using the program SENIT ModelFit. This program which was developed at the Norwegian research institution SINTEF, utilizes an algorithm based on a modified extended Kalman filter (Schei, 1997) to estimate states and parameters in nonlinear state space models. An outer SQP-type optimization loop optimizes the initial values for the parameters and states by minimizing the difference between the measured output, here measured alumina concentration and

total cell voltage drop, and the corresponding simulated model output.

The dispersion parameters $k_{1\rightarrow2}$ and $k_{2\rightarrow3}$, the mass transfer coefficient k_{mtf}, the mass of electrolyte in a control volume M_e and the initial conditions for anode-cathode distance, δ_0 were estimated simultaneously by fitting the model response to the measured data from experimental run 1. Reasonable estimates of initial undissolved and dissolved alumina concentration were found by manual comparison with the measured alumina concentration. The optimal model response for experimental run 1 is shown in Fig. 3.
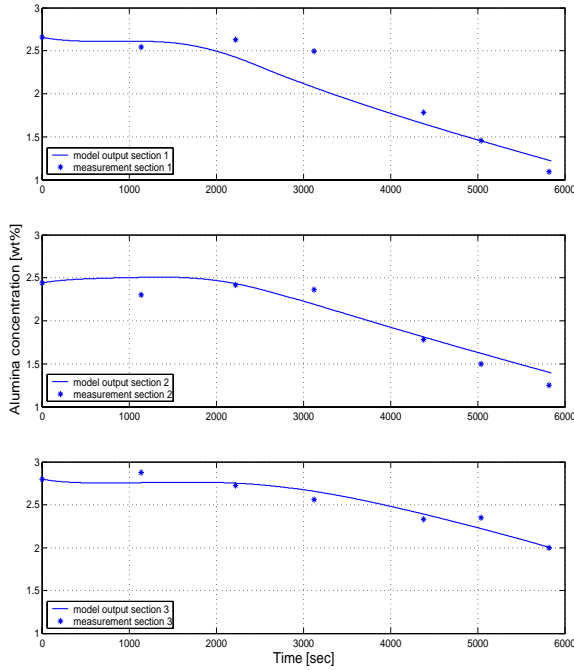

Fig. 3. Estimation of parameters and initial states. Measured alumina concentration compared to model output (no Kalman filter update) for experimental run 1 using the optimal parameter values and initial states.

The parameters describe physical properties of the process and the values are expected to vary somewhat over time and from cell to cell. The optimal parameter values estimated using data from experimental run 1 proved to yield acceptable model response also when applied to input data from the other two experiments. Minor adjustments of the mass of electrolyte M_e, and the dispersion parameters further improved the model response. This was expected since the mass of electrolyte are known to vary and the magnitude of the dispersion parameters depends on the actual convection flow pattern in the cell at the time.

The initial conditions for anode-cathode distance had to be optimized for each experimental run in order to get acceptable results. This was done by fitting the cell voltage drop estimated by the model to the first few cell voltage measurements

in the relevant experiment. Fig. 7 illustrates how the initial values for anode cathode distance affect the estimate of alumina concentration through the Kalman filter. Bad initial values are usually indicated by a difference between calculated model voltage drop and measured cell voltage drop, and this results in a large prediction error.

5.2 State estimation and fault detection

In normal operation alumina concentration is measured only about once a day and only in one position in the cell. A good model should therefore be able to give reliable estimates also when no concentration measurements are available. After a set of acceptable parameter values and initial conditions are identified using both measurements of alumina concentration, cell voltage, anode currents and correct input data, the alumina concentration is estimated using measurements of cell voltage, anode current distribution and the input data stored in the process database only. Based on the difference in modeled and measured output, the alumina model estimate is updated through an extended Kalman filter algorithm (Schei, 1997) implemented in Matlab.

Earlier results (Jakobsen *et al.*, 2001) indicate that using the measurements of anode currents and voltage to update the model output in a Kalman filter did not improve the estimate of alumina concentration considerably for the fault free input case. Here the effect of using the Kalman filter for state estimation when the input feed rate to the model is faulty is investigated. For example, if one of the feeders is malfunctioning, the process control system may assume that the feed rate is normal while in fact severe disturbances in feed rate take place. This is the case for the experimental data set 1 and 2. Fig. 4 and Fig. 6 show how the estimate of alumina concentration for faulty input feed rate is improved through the Kalman filter. By examining the difference between the model output (no Kalman filter update) and the estimate from the Kalman filter as the actual alumina concentration in the cell decreases, an indication of abnormal alumina distribution is observed early enough in experimental run 1 and 2 to prevent the oncoming anode effect. The results for experimental run 3 were not so good. As is illustrated in Fig. 5, the estimate of alumina concentration was disturbed by an anode beam movement and did not follow the measured value accurately afterwards.

6. CONCLUSIONS AND DISCUSSION

The rather crude model for estimation of alumina concentration in an aluminium electrolysis cell

does give acceptable model response when the parameters and initial conditions are fitted to the experimental data. Since the model is reduced to three control volumes and all mass transport is modeled as dispersion, the problem of modeling the unknown convection flow pattern in the cell is eliminated. The two dispersion parameters are fitted to the experimental data, indirectly describing the effect of convection on alumina distribution.

Using the model for detection of abnormal feed rates gave promising results. When the actual concentration of alumina in the cell was low, the effect of assuming an incorrect feed rate was reduced when the concentration estimates were updated through the Kalman filter. By examining the difference between the model output and Kalman filter estimate information about abnormal changes in alumina distribution could be gained early enough in some cases to prevent an oncoming anode effect. However, some points proved to be extremely important to get good results:

- As is seen in Fig. 7 good initial values for anode-cathode distance is important. Since anode-cathode distance directly influences the inter-electrode resistance and thereby cell voltage, a poor initial estimate will result in a difference between estimated and measured cell voltage. The Kalman filter will try to compensate for the large prediction error by adjusting alumina concentration. A bad initial estimate for anode-cathode distance might give a new estimate of alumina concentration that differs significantly from the actual value.
- Tuning of the Kalman filter matrices. The two matrices V and W representing the process and measurement noise respectively must be supplied to the Kalman filter algorithm. Tuning of these matrices are crucial to get good results. If too much emphasis is given to the measurements, the estimates may reflect measurement noise not related to alumina distribution. A problem with estimator stability was observed for certain combinations of V and W. The cause of this instability is a topic for further work, but may well be a combination of the strong nonlinearity of the process and the rather crude model
- The effect of anode beam movement. The model value of anode-cathode distance is not updated in the Kalman filter and can only be changed by moving the anode beam. Thus, the anode current distribution could be expected to remain relatively constant as all anodes in a cell experience the same change in anode-cathode distance. In practice however, this is often not the case. First, a movement of the anode bream usually implies that something is less than optimal in the cell

to begin with. Second, we lack information of the processes going on in the electrolyte that may affect anode current distribution. For example, movement of the anode beam may influence the flow pattern in the cell. As is indicates in Fig. 5 a re-optimization of the anode-cathode distance often seem to be required after an anode beam movement.

6.1 Further work

The experiments considered in this paper all involve rather large disturbances in feed rate that seldom occur in normal operation. Further work should involve validating the model against normal operation data focusing on detection of minor feed disturbances and oncoming anode effects.

7. ACKNOWLEDGMENTS

REFERENCES

Bearne, G.P. (1999). The development of aluminium reduction cell process control. *Journal of the Minerals & Materials Society* **51**(5), 16–22.

Haupin, W. (1998). Interpreting the components of cell voltage. In: *TMS Light Metals 1998. Proceedings of the Annual Meeting in the Minerals, Metals and Materials Society.* pp. 531–537.

Jakobsen, S.R., K. Hestetun, M. Hovd and I. Solberg (2001). Estimating alumina concentration distribution in aluminium electrolysis cells. In: *Preprints of the IFAC MMM2001.* IFAC MMM. Tokyo, Japan. pp. 253–258.

Rye, K.Å., M. Königsson and I. Solberg (1998). Current redistribution among individual anode carbons in a hall-heroult prebake cell at low alumina concentrations. In: *TMS Light Metals 1998. Proceedings of the Annual Meeting in the Minerals, Metals and Materials Society.* pp. 241–246.

Schei, T.S. (1997). A finite-difference method for linearization in nonlinear estimation algorithms. *Automatica* **33**(11), 2053–2058.

Solheim, A. (1998). Reviderte aktivitetsdata for NaF, AlF_3 og Al_2O_3. Rapport for PROSMAT, prosjekt P3.7 cellespenning (In Norwegian). Technical report. SINTEF.
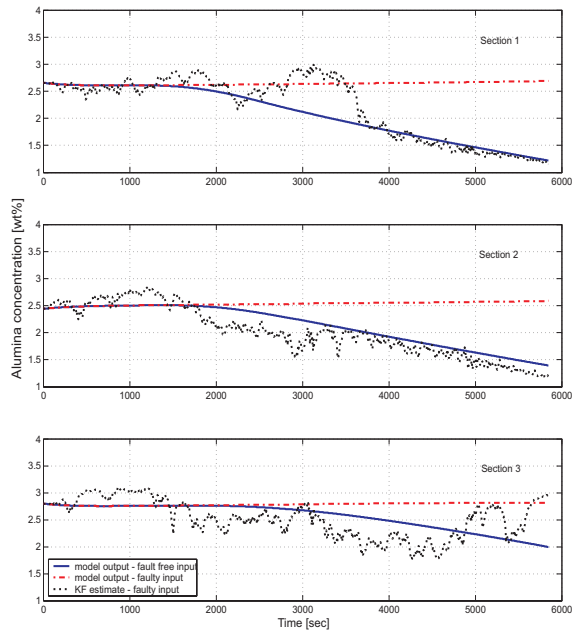
Fig. 4. Detection of faulty feed rate, experimental run 1. Solid line represents model output for the correct input feed rate (feeder F1 closed down at $t = 1000\,\mathrm{sec}$) . $-.-$ gives model output for faulty feed rate (assume that both feeders have normal feed rate). $\cdots$ represents the alumina concentration estimate from the Kalman filter when the input feed rate is faulty.
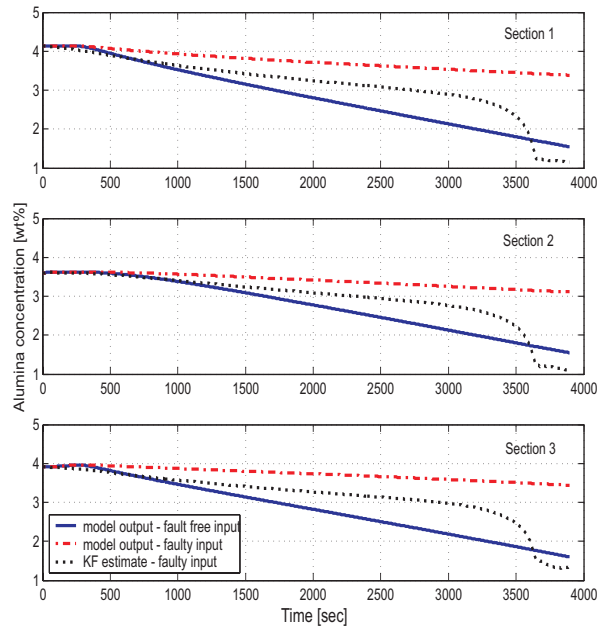

Fig. 6. Detection of faulty feed rate, experimental run 2. Solid line represents model output for the correct input feed rate (feeder F1 and F2 closed down) . $-.-$ gives model output for faulty feed rate (assume that both feeders have a feed rate equal to 50% of normal feed rate). $\cdots$ represents the alumina concentration estimate from the Kalman filter when the input feed rate is faulty.
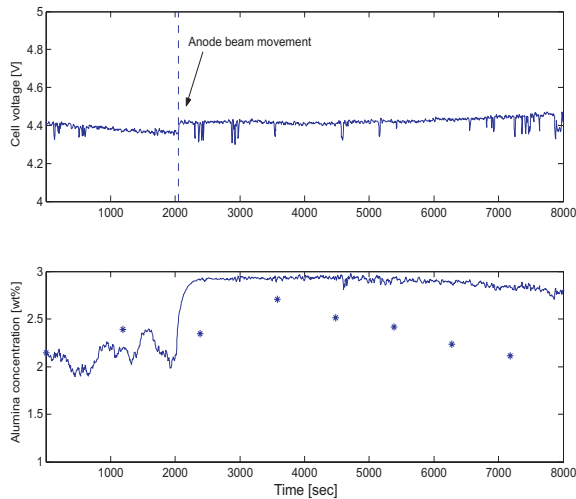

Fig. 5. Effect of anode beam movement on alumina concentration estimate. The first plot shows measured cell voltage drop. The second plot shows the Kalman filter alumina concentration estimate for section 1 (solid line) and corresponding measured values (*) for experimental run 3.
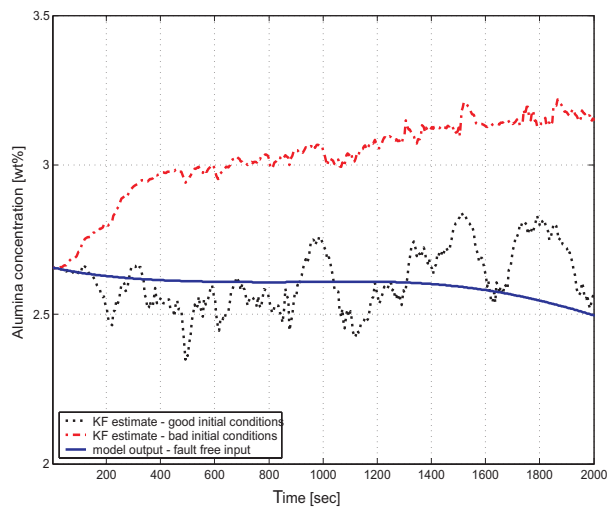

Fig. 7. The importance of initial anode cathode-distance. $-.-$ and $\cdots$ are the Kalman filter estimates for two sets of initial values for anode-cathode distance for experimental run 1. The solid line is the fault free model output.